Role of the benzodioxole group in the interactions between the natural alkaloids Chelerythrine and Coptisine and the human telomeric G quadruplex DNA. A multiapproach investigation.

F. Papi,[1,2] M. Ferraroni,[1] R. Rigo,[3] S. Da Ros,[3] C. Bazzicalupi, [1]* C. Sissi[3]* and P. Gratteri[2]*

1 Department of Chemistry "U. Schiff", Univ. of Florence, via della Lastruccia 3, 50019 Sesto F.no, Florence Italy

2 Department Neurofarba - Pharmaceutical and Nutraceutical Section and Laboratory of Molecular Modeling Cheminformatics & QSAR, University of Florence, via U. Schiff 6, 50019 Sesto F.no, Florence Italy

3 Department of Pharmaceutical and Pharmacological Science, Univ. of Padua, via F. Marzolo 5, 35131 Padua, Italy

Abstract

The binding properties towards human telomeric G-quadruplex of the two natural alkaloids Coptisine and Chelerythrine were investigated and compared with respect to those of their parent compounds Berberine and Sanguinarine. A variety of investigation methods were used, e.g. spectroscopic techniques, X-ray diffraction analyses and molecular modelling. Spectroscopic studies showed modest, but different rearrangements of the DNA-ligand complexes which can be clearly referred to the peculiar stereochemical features for these two alkaloids, in spite of the similarity of their skeletons. In fact, the closure into a dioxolo ring of the two methoxy functions rises the efficiency of Coptisine and Sanguinarine in comparison to Berberine and Chelerythrine, and the overall stability trend result to be Sanguinarine > Chelerythrine ≈ Coptisine > Berberine. Accordingly, the X-ray diffraction results confirmed the involvement of the benziodioxolo groups in the Coptisine/DNA binding by means of π···π, O···π and CH···O interactions. Similar information is provided by modelling studies, which, additionally, evidenced reasons for the quadruplex vs double-helix selectivity shown by these alkaloids. Thus, findings of this study shed light on the key role of the benzodioxolo moieties in strengthening the interaction with the G4-folded human telomeric sequence and pointed out the better G4 stabilizer properties of the benzophentridine scaffold with respect to the protoberberine one. Moreover these results were found able to explain the ds vs. G4 selectivity trend of the investigated alkaloids.

Introduction

The interest toward G-rich DNA sequences, able to fold in the so-called G-quadruplex structures, tremendously grew during the last decades. Among the several G-quadruplex forming sequences identified in human genome, the telomeric DNA is one of the most studied [1,2]. Telomere are found at the end of chromosomes and in eukaryotic cells are formed by (TTAGGG) repeats. Here, the 3' terminal is present as a protruding single strand and represents the substrate of telomerase. This enzyme is a ribonucleoprotein activated in more than 80% of tumors, where it maintains telomere length by a reverse transcriptase

activity. Folding of the 3' protruding single-stranded telomeric DNA into a G-quadruplex structure is known to inhibit telomerase activity and it has recently been suggested as an innovative therapeutic anticancer strategy [2]. Consequently, ligands that bind and induce telomeric G-quadruplexes are extensively explored as potential anticancer drugs. Since telomeric activity is predominantly present in cancer cells, in principle, they are expected to be targeted agents with reduced side effects [3-6]. On the other hand, good G-quadruplex binders usually have structural and chemical features that are very similar to those requested to double stranded DNA intercalators, i.e. a large aromatic surfaces and, possibly, positive charges. Thus, large research efforts are directed to rationally prevent potential off-target effects.

A number of compounds have been shown to either stabilize G-quadruplex structures or promote their formation. Among them, natural compounds are an important resource due to the considerable variability in their chemical structure, their wide availability from natural sources, the low cost of their extraction processes, and most importantly, their general low toxicity [7].

The plant-derived alkaloids, such as isoquinoline derivatives, belong to one of the most widespread building blocks and possess prominent biological and pharmacological activities, with a role of remarkable importance in the contemporary biomedical research and drug discovery programs [8-11]. Antimicrobial, anti-inflammatory, anti-oxidative and anti-diabetic activities have been reported for compounds belonging to this group [12-14]. In addition, anticancer properties are ascribed to their ability to form complexes with DNA and RNA [9,13,15] and also to their antimicrobial effects on tumorigenic microorganisms as well as to their potential regulation of oncogene and carcinogenesis-related genes expression [16].
Up to now, however, most of the studies carried out on the DNA telomeric G-quadruplex/alkaloids complexes, have mainly focused on the planar isoquinoline alkaloid Berberine and its protoberberine derivatives, as well as on the benzophenanthridine alkaloid Sanguinarine (Scheme 1) [17-20]. Coptisine (6,7-Dihydro-bis(1,3)benzodioxolo (5,6-a:4',5'-g)quinolizinium) and Chelerythrine (1,2-dimethoxy-12-methyl- [1,3]benzodioxolo[5,6-*c*]phenanthridin-12-ium) are structural analogs of Berberine and Sanguinarine, respectively. The two partners of each homologous pair differ only for the overall number of methylene dioxy or methoxyl substituents (Scheme 1). They are known to be DNA binders, with cytotoxic and apoptotic abilities which make them interesting also for modulation of multidrug resistance in several cancer cells [21]. Moreover, recent in solution and modeling investigations carried out on Chelerythrine, provided evidence of its binding ability towards telomeric DNA [22-25].

We previously reported that Sanguinarine, bearing two methylene dioxy moieties, was a better stabilizer with respect to Berberine for the G-quadruplex structure assumed by the human telomeric sequence [20]. Here, we investigated the binding properties towards human telomeric G-quadruplex of the two analogues compounds Coptisine and Chelerythrine, by using different spectroscopic techniques, XRD and molecular modelling.

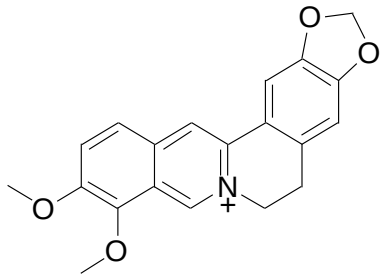

Berberine

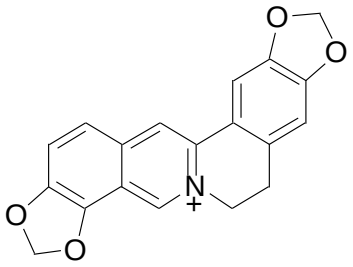

Coptisine

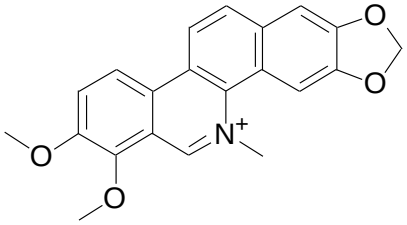

Chelerythrine
iminium form

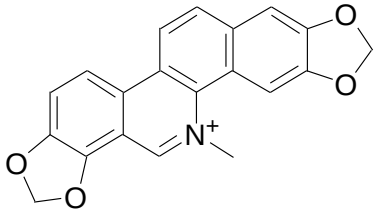

Sanguinarine
iminium form

Scheme 1

Results and Discussion

In potassium containing solutions, both Chelerythrine and Coptisine stabilize G4-folded human telomeric sequence to a significant extent. In particular, by a fluorescence melting assay we pointed out that Chelerythrine and Coptisine have quite similar effects on the telomeric G4 and induce intermediate thermal stabilizations (ΔTm) when referred to the previously reported parent compounds Sanguinarine and Berberine (Figure 1 panel a) [20]. The resulting overall stability trend is Sanguinarine>Chelerythrine≈Coptisine>Berberine. Chelerythrine being slightly more efficient than Coptisine. Thus, the closure of the two methoxy functions into a dioxolo ring rises the efficiency of Coptisine and Sanguinarine in comparison to Berberine and Chelerythrine, respectively, in line with a previously reported evidence indicating that the presence of benzo[1,3]dioxole groups in alkaloid derivatives promotes the interaction with G-quadruplex structures from human telomeric DNA [26].

In the same experimental conditions, all four alkaloids share a significantly reduced effect on a random double helix DNA, thus foreseeing a potential selectivity for the tetrahelical arrangement (Figure 1 panel b).

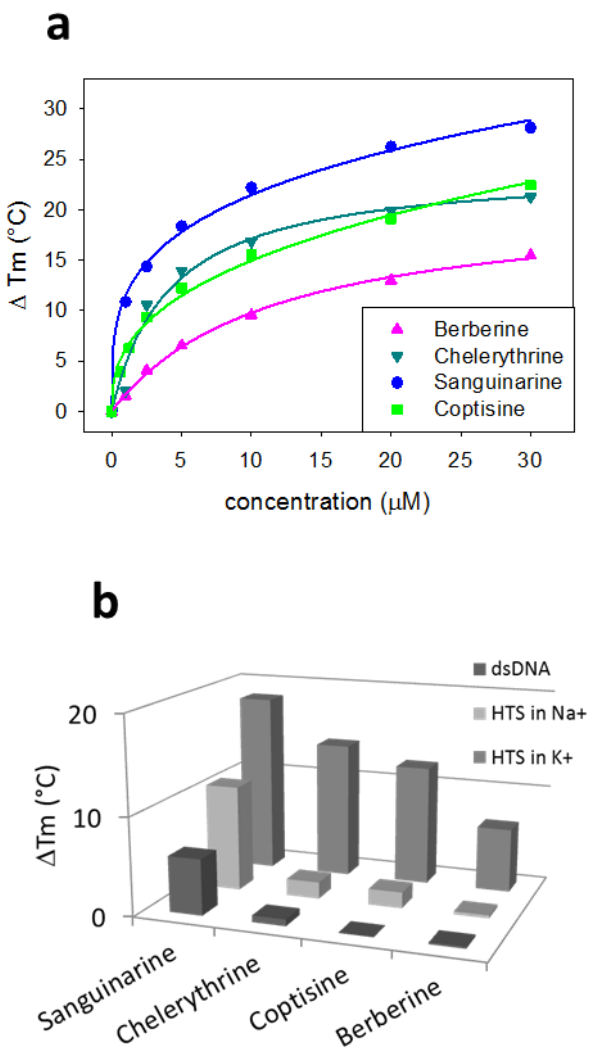

Figure 1: (a) Thermal stabilization of the human telomeric sequence HTS in the presence of increasing concentrations of tested alkaloids in 10 mM LiOH; 50 mM KCl, pH 7.5. (a) Shift of the melting temperature induced by 5 μM ligands on dsDNA or on HTS in50 mM KCl or 50 mM NaCl is reported. (data for Berberine and Sanguinarine taken from ref. 20).

The presence of K^+ or Na^+ in the buffer, profoundly alters the G-quadruplex folding of the telomeric sequence shifting it from a hybrid towards an antiparallel arrangement, respectively. For Chelerythrine, by using different techniques Bai et al. found an affinity ranking order for telomeric DNA corresponding to hybrid K^+ >> basket Na^+ [25]. This same trend is here confirmed for all tested alkaloids resulting in a relevant preference for the hybrid conformation (Figure 1 panel b).

However, it is well known that the so called hybrid form assumed by the telomeric sequence in K^+ containing solutions, actually comprises several distinct folded species in equilibrium with low energetic barriers [27]. Among them two different 3 + 1 foldings, named hybrid 1 and hybrid 2, are highly

represented in solution; their relative abundance is a function of the length and sequence of the nucleic acid [28].

With this issue in mind, we decided to deeply investigate if the preferential recognition of the K^+ induced G-quadruplex observed for Chelerythrine and Coptisine is in some way dependent on the folding assumed by the telomeric sequence. To this aim, we performed a FID competition assay by using two different sequences, namely Tel26 and wtTel26, known to fold into a prevalent H1 or H2 hybrid form, respectively. As fluorescent probe for these G4 structures, we used Thiazole Orange that shows comparable binding affinity for both of them. As shown in Table 1, both Chelerythrine and Coptisine were able to displace the dye from the folded telomeric sequences. Coptisine showed lower efficiency in comparison to Chelerythrine on both substrates, mostly on H1 hybrid form. Interestingly, for this compound, a more significant preference for the H2 form emerged.

TABLE 1 - EC_{50} derived by FID for the interaction of Chelerythrine and Coptisine with the hybrid 1 (H1) and hybrid 2 (H2) folding of telomeric DNA.

	H1	**H2**	**H2 vs H1**
Chelerythrine	2.59 ± 0.10 μM	3.75 ± 0.24 μM	0.7
Coptisine	12.01 ± 0.82 μM	5.93 ± 0.36 μM	2.0

In line, CD titration of the two G4 forms with the tested alkaloids confirmed their interaction with the two DNA templates as supported by a conserved increment of the positive band centered at 295 nm and a reduction of the 260 nm band (Figure 2). However, subtle differences in the binding modes of the two DNA templates by the two ligands emerged. Indeed, at saturations the final CDs are slightly different thus actually supporting a modest rearrangement of the DNA-ligand complex and suggesting that the G-quadruplex binding site for the two alkaloids might not perfectly overlap.

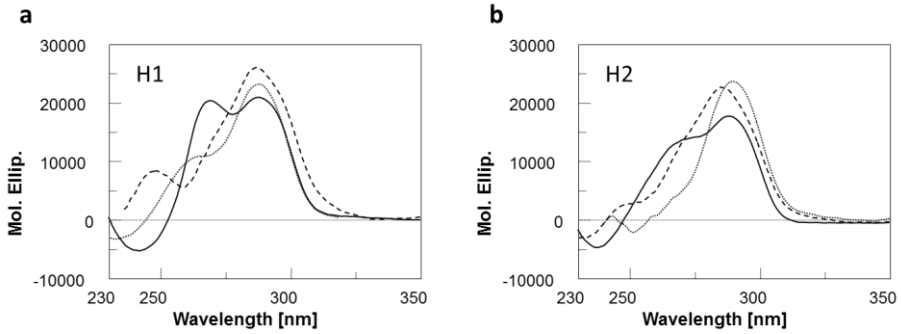

Figure 2: CD spectra of 4 μM (A) Tel26 (H1) and (B) wtTel26 (H2) in 10 mM Tris, 50 mM KCl, pH 7.5, in the absence (solid lines) or in the presence of 40 μM Chelerythrine (dashed lines) or Coptisine (dotted lines)

A similar modulation in DNA recognition occurs also on dsDNA. Indeed, despite a reduced interaction of the two alkaloids with this template in comparison to the G4, distinct UV and CD features characterize the two alkaloid-dsDNA complexes (Figure S1 ESI). These differences can be clearly referred to the peculiar stereochemical features for these two alkaloids, in spite of the similarity of their skeletons. Indeed, previously reported crystallographic data indicate that whereas Chelerythrine interact with DNA in its planar and charged iminium form (Scheme 1), Coptisine is not planar and features a 18° dihedral angle between its phenyl and quinoline moieties [29].

To further highlight the molecular basis governing the binding of Chelerythrine and Coptisine on telomeric G-quadruplex, molecular modeling investigations were carried out on the two structurally characterized hybrid arrangements associated to the Tel26 (H1) and wtTel26 (H2) telomeric sequences (see Methods section). Despite Chelerythrine adopts in its adduct with H1 a not completely flat conformation (naphthalene and benzodioxolo moieties form a dihedral angle of about 16°), it is very well placed on the quartet formed by G4-G10-G18-G22 residues (Figure 3) establishing π-π interactions mainly with the G22 guanine and with G4 (interplanar distances ranging from 3.4 to 3.9 Å). The flanking A3 adenine residue wraps over the ligand. The overall binding is then reinforced by a salt-bridge involving the charged ligand nitrogen, which is located at 3.5 Å from a phosphate oxygen of G22 (Figure 3b).

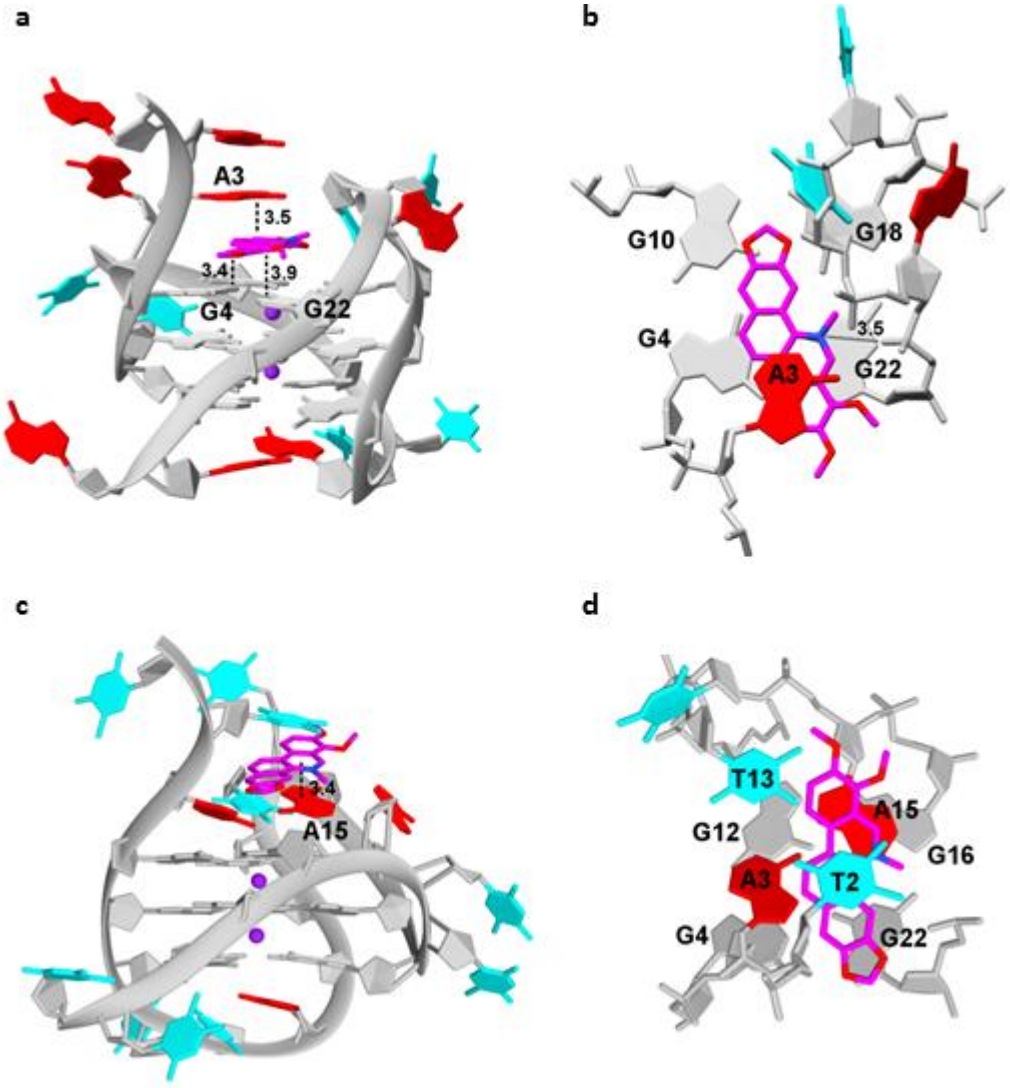

Figure 3 - Calculated conformers for the complexes of Chelerythrine with H1 - lateral (a) and top view (b) – and with H2 - lateral (c) and top view (d) –. (adenine, tymine and guanine residues are in red, cyan and gray, respectively)

In the adduct formed with H2, Chelerythrine is not in direct contact with the guanine quartet formed by G4-G12-G16-G22 residues, but it gives face to face stacking (3.4 Å interplanar distance) with the adenine-A15 (Figure 3 c,d).

In the lowest energy conformer found for the Coptisine/H1 adduct (Figure 4 a,b), the most important interactions seem to be two H-bonds involving the two dioxolo groups and A21 adenine (2.05 Å) or T7 thymine (2.18 Å). These two interactions fix the molecule in a quite bent conformation (about 23° between the quinoline and benzodioxolo group) thus preventing the optimal stacking with the 5'-end tetrad. In fact, the quinoline moiety stacks with just the G10 guanine (3.7 Å interplanar distance). Moreover, CH···π contact (2.7 Å) is formed between the methylene group from a benzodioxolo and A9 adenine (Figure 4a).

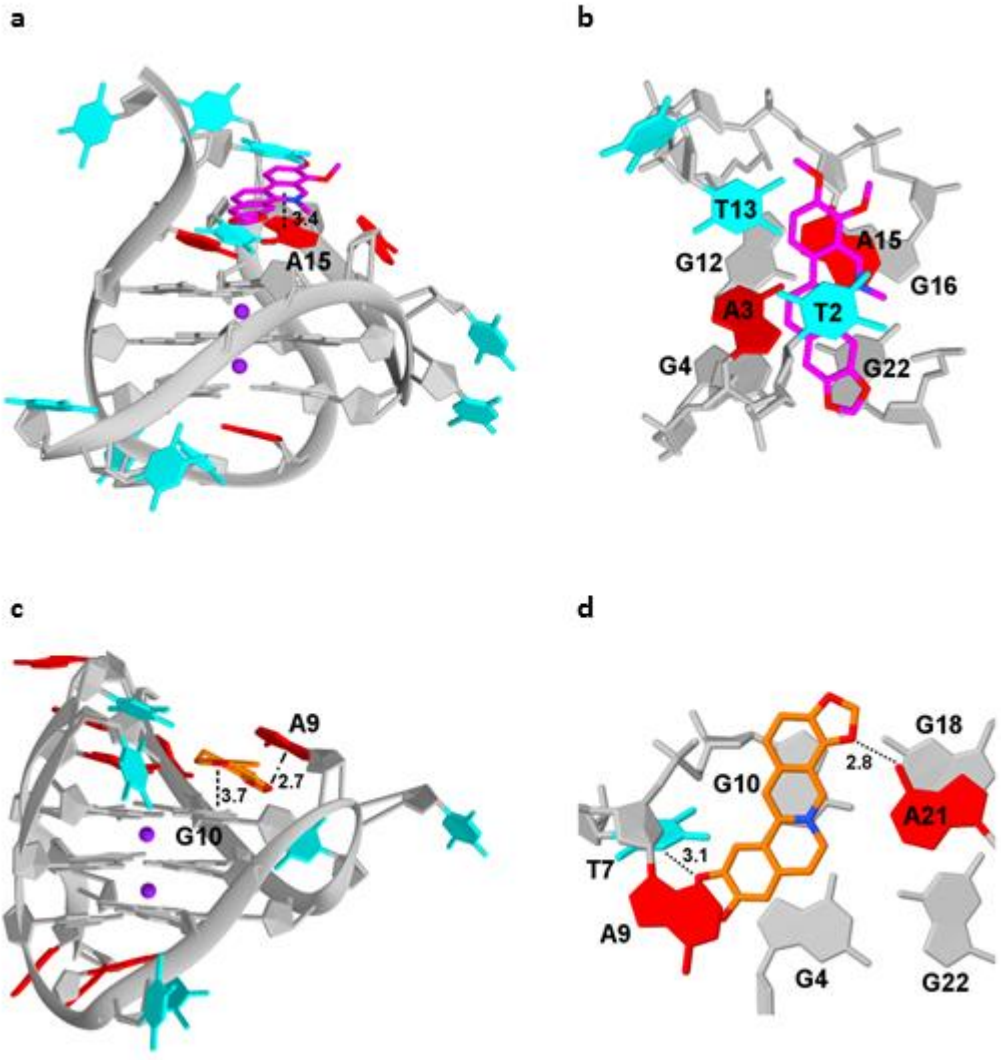

Figure 4 - Calculated conformers for the complexes of Coptisine with H1 - lateral (a) and top view (b) – and with H2 - lateral (c) and top view (d) – (adenine, tymine and guanine residues are in red, cyan and gray, respectively)

A less bent conformation is instead assumed by Coptisine in the adduct formed with H2 (about 17° between the quinoline and benzodioxolo group -Figure 4 c,d). In this adduct the ligand reaches the guanine quartet, giving a stacking interaction with G22 and G16. (interplanar distances 3.7 Å). In a similar fashion as for Chelerythrine, A15 flanking base at 5'-end wraps Coptisine establishing a π-stacking interaction at about 3.6 Å interplanar distance.

Basing on these findings the Coptisine scaffold seems better suited for the H2 arrangement of the telomeric DNA thus supporting the solution study's results which highlight the remarkable preference of Coptisine for the H2 over H1 folding.
Interesting comparison can be derived for the interaction behavior of these two alkaloids with respect to their parent compounds Berberine and Sanguinarine. In fact, it is noteworthy that stable poses not involving the guanine quartets have been found for both the benzophenantridine compounds Sanguinarine and Chelerythrine. Indeed, in a previously reported study, Sanguinarine was found to act as groove binder of the hybrid arrangement [20]. Moreover, NMR experiments pointed out that in the case of the basket arrangement, Sanguinarine locates close to the loop residue A7. These binding preferences can explain the low double helix over G-quadruplex selectivity especially found for Sanguinarine. On the other hand, Berberine and Coptisine, invariably interact with the quartet and are able to well discriminate double helix vs. quadruplex structures.
In addition, solution data indicate that the presence of the two benzodioxole rings rises the stability of Coptisine and Sanguinarine adducts with respect to those formed by Berberine and Chelerythrine, respectively. In line with these observations, modelling results evidence that the methylene dioxy group is involved in the interaction with the target only in the case of Sanguinarine and Coptisine while Berberine and Chelerythrine, bearing two methoxy groups, lack this kind of contact.

To fully explore the structural arrangement of adducts formed by Coptisine and Chelerythrine with the telomeric DNA, crystallization screenings were carried out for both alkaloids by using the Tel12 and Tel23 sequences, which afford bimolecular and monomolecular G4 structures, respectively. Crystals suitable for X-ray diffraction analysis were obtained only for the adduct of Coptisine with the 12-mer human telomeric sequence d(TAGGGTTAGGGT). The crystal structure is built up by parallel stranded-bimolecular quadruplexes and ligand molecules in 1:1 molar ratio. Each quadruplex unit contains the three planar stacked G-quartets, 3.4 Å apart from each other, typical of human telomeric quadruplex. As shown in Figure 5, the quadruplex is formed by two symmetry independent chains, where the TTA sequences connecting the guanine tracts form propeller loops which protrude outwards. The propeller TTA loops can be described as type 5 and type 1 (subtype 2), according to the analysis reported by Neidle and coworkers [30].
Analogously to the previous reported telomeric quadruplex structures, monovalent K^+ cations are found in the internal channel located between two adjacent guanine tetrads, 2.7-3.0 Å apart from the eight O6 carbonyl oxygens which determine an antiprismatic coordination sphere.
One of the 3'-end terminal thymine residue (T12, light gray chain in Figure 5A) stacks on the underlying G-quartet, while the other (T24, dark gray chain in Figure 5A) protrudes outside providing a binding point with adjacent symmetry related quadruplexes.

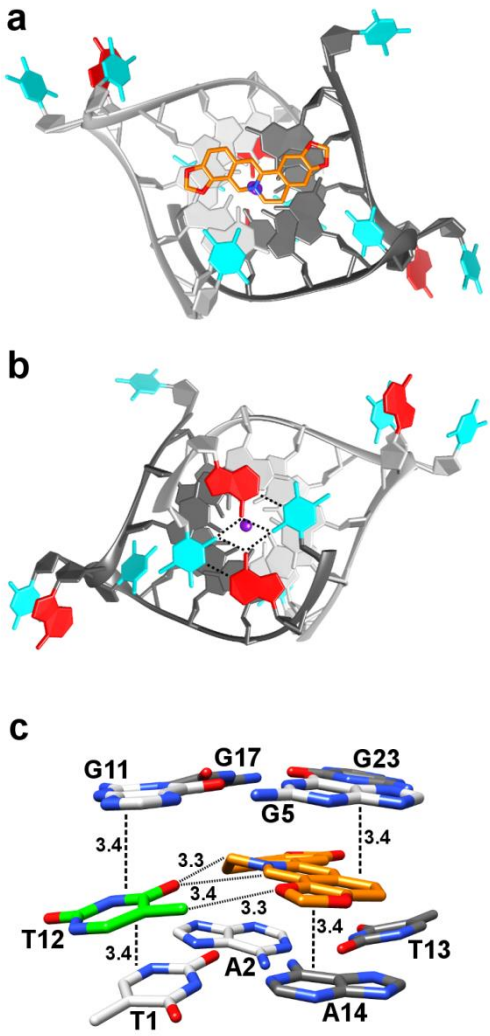

Figure 5- Crystal structure of the Tel12/Coptisine adduct. Top view of the T12 residue and the Coptisine molecule stacked on the 3'-end tetrad of the target molecule (a) and of the TATA quartet at the 5'-end tetrad (b). View of the binding site (c). Dotted lines indicate the H-bond contacts between the thymine and adenine residues (distances range from 2.7 Å to 3.1 Å). The two symmetry independent Tel12 chains are light and dark gray colored. T and A residues are colored in cyan and red, respectively.

As the 5'-end is concerned, the thymine and adenine residues from the two chains interact via Watson-Crick H-bonds forming an additional tetrad which stacks on the G-quartet (Figure 5B). Differently from the G-quartets, which are formed by four almost perfectly coplanar guanines, in the TATA platform each adenine forms with the adjacent thymines dihedral angles with values falling in the range 14-23°. The quadruplex units are head-to-tail disposed in column which grow along the 4-fold screw axis, with the Coptisine molecule and the T12 residue sandwiched between the 3'-end G-quartet and the 5'-end TATA tetrad from the following quadruplex unit (ESI - Figure. S3).

As a consequence, the binding site of Coptisine is defined by the 3'-end G-quartet and the 5'-end TATA platform belonging to adjacent units in the column, with the alkaloid being approximately 3.4 Å apart from each quartet (Figure 5c). Coptisine is asymmetrically placed respect to the four guanines and in contact with only two of them, each belonging to a different chain. On the other side, Coptisine gives contacts with the two adenine residues of the 5'-end TATA platform. The cationic nitrogen is located approximately in line with potassium ions in the central channel, and points towards one of the O4 carbonyl oxygen of the

T12. Interestingly, this thymine residue and the Coptisine interact via CH···O hydrogen bonds (C…O distances 3.3 Å).

In the present complex Coptisine is quite planar, featuring a 13° dihedral between the phenyl and the quinoline groups (Scheme 1). QM calculations have demonstrated that Coptisine can assume bent conformations [29] and among these, the most stable is characterized by the greater dihedral angle (about 30°). Interestingly, this bent conformation was found to bind an unusual C:G:G:C tetrad formed by adjacent double helices of CGATCG sequence in the crystal structure of the CGATCG/coptisine adduct (Figure 6 and Figure S4 - ESI) [29]. As shown in Figure 8, in the binding site Coptisine is stabilized by π···π and O···π interactions, so confirming, together with the presence of CH···O analogous to the interaction evidenced in Figure 5C, the involvement of the benzodioxolo groups in the Coptisine/DNA binding.

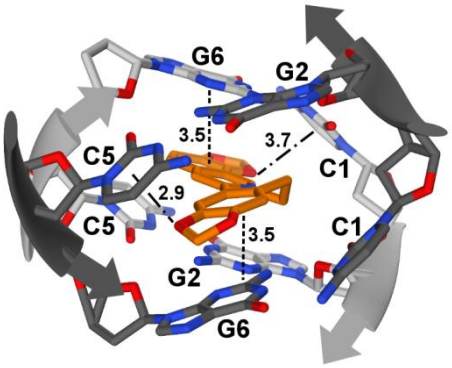

Figure 6 - C:G:G:C platforms defining the binding site for Coptisine in the CGATCG/coptisine adduct (data from ref. 27).

Thus, the almost planar conformation assumed in the solved structure is most likely due to the π-stacking interactions established with both 3'-end GGGG and 5'-end TATA quartets. The planar conformation is usually found in the solid state structures of alkaloids belonging to the protoberberine family reported in the Cambridge Structural Database [31]. In these cases, the crystal packing forces play a relevant role influencing the overall conformation of the crystallized species.

Among the crystal structures previously reported for telomeric quadruplex in complex with ligand, that of the adduct formed by the Tel12 sequence and BRACO-19 is the most similar to the Coptisine adduct. Actually, also the BRACO ligand in its binding site is in contact with a thymine residue, both ligand and thymine being sandwiched between a G-quartet and a TATA platform of symmetry related G-quadruplex units. On the other hand, the most interesting difference between the two structures is that in the BRACO complex the residues giving the TATA platform belong to two head-to-tail quadruplexes, particularly a 3'-end thymine and the 5'-end ATA group, while in the Coptisine/Tel12 adduct all the residues forming the TATA platform belong to and stack on the same G-quadruplex. In line with this finding the TATA platform evidenced in our crystal structure could be maintained also in the isolated quadruplexes present in diluted solution, thus constituting a potential binding site.

To analyze the possible formation in diluted solution of a sandwich comprising two G4 units and one Coptisine, we performed EMSA and CD experiments . The formation of such kind a sandwich was ruled out in diluted solution (up to 10 μM oligonucleotide) both in the absence and in the presence of MPD, the same cosolvent used to obtain the crystal. Indeed, on gel (ESI, Figure S5) we never solved the dimer that is expected to have a reduced electrophoretic mobility due to its increased hydrodynamic volume. Conversely, the cosolvent was actually able to induce the complete folding of the oligonucleotide into a G-

quadruplex. In these conditions, the corresponding CD is characterized by two well resolved main positive bands centered at 295 and 260 nm. Although the G-quadruplex- Coptisine interaction was evidenced by the increment of the CD bands intensities, the maxima/minima wavelengths were preserved up to a 10-fold excess of ligand vs G4, so confirming that Coptisine is not altering significantly the overall geometry of the nucleic acid in our experimental conditions (Figure 7).
Nevertheless, it is interesting to note that crystal structures containing A/T-based platforms analogous to what found in our Coptisine/Tel12 complex, have been also recently observed by Neidle and coworkers [32]. As in our structure, the A/T-based platforms are formed by residues belonging to the same chain. Moreover, the platforms are stacked on the telomeric G4 in a very similar way to what found in our Coptisine/Tel12 complex. Noteworthy, the A/T-based platforms constitute the junction between a human telomeric quadruplex and its corresponding duplex and, consequently, can be regarded as a potential binding site.

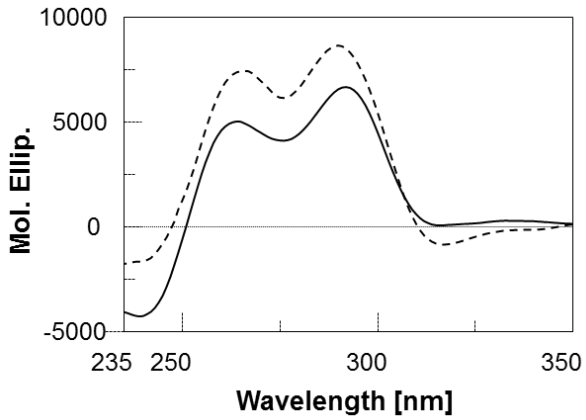

Figure 7 - CD spectra of 8 μM Tel12 recorded in 10 mM Tris, 50 mM KCl, 40 % MPD in the absence (solid line) or presence (dotted line) of 40 μM Chelerythrine.

Conclusion

The two studied alkaloids Chelerythrine and Coptisine are able to bind the human telomeric sequence arranged in quadruplex foldings. Similarly to the data previously reported for the parent compounds Sanguinarine and Berberine, the ΔTm values here reported point out the slightly higher stabilization ability of Chelerythrine over Coptisine and the benzophenanthridine scaffold is confirmed to better interact with the telomeric G quadruplex than the protoberberine one. The Sanguinarine > Berberine stabilizing trend was previously interpreted as a consequence of the different degree of planarity and/or π-delocalization between the scaffolds of the two ligands. The here obtained results clearly highlights that planarity is not the only important feature, and other aspects should be taken into account. Indeed, comparing ligands characterized by the same scaffold, stronger interactions are always found when an additional benzodioxolo ring replace the two methoxy functions (stability trend Sanguinarine > Chelerythrine and

Coptisine > Berberine). Interestingly, both in silico modelling and X-ray diffraction analysis demonstrate that the benzodioxolo groups of Coptisine can be involved in contacts which stabilize the formed adducts.

The theoretical investigation and the structural analysis of the Coptisine/Tel12 complex, as well as the adduct Berberine/Tel23 already present in literature, show that both ligands are able to give quite good stacking on the guanine tetrads. In the case of Chelerythrine, the ligand can establish interactions with both the quartet and loop residues in that making it more similar to the Sanguinarine, the less selective among these four alkaloids. In conclusion, our work has shed light on the interaction between human telomeric G-quadruplex folding and selected natural alkaloids with interesting anticancer activity. The results show that Coptisine is the most valuable candidate for further studies as G4-binding compound, moreover we have obtained important clues for the design of new G-quadruplex ligands with better binding properties.

Methods

Materials. All synthetic DNA were provided by Biosense (wtTel26 (H2) (5'-TTAGGGTTAGGGTTAGGGTTAGGGTT-3'), Tel26 (H1) (5'-AAAGGGTTAGGGTTAGGGTTAGGGAA-3'), HTS (5'-Dabcyl-AGGGTTAGGGTTAGGGTTAGGGT–FAM-3') and scT22 (5'-Dabcyl-GGATGTGAGTGTGAGTGTGAGG paired to the complementary strand labelled with FAM at 3') and by Jena Bioscience (Tel12 (5'-TAGGGTTAGGGT-3') and Tel23 (5' – TAGGGTTAGGGTTAGGGTTAGGG -3')). Before use they were annealed in the required buffer. ctDNA was purchased from Sigma-Aldrich.

CD analyses

Circular dichroism spectra were recorded in the 230-350 nm range on a Jasco J-810 spectropolarimeter equipped with a Peltier temperature controller using a 10 mm path-length cell. DNA substrates were prepared at 4 μM (strand concentration) by annealing in 10 mM Tris, 50 mM KCl, pH 7.5 with or without 40% MPD. Spectra were acquired in the absence or presence of increasing concentrations of ligands (0-80 μM). Observed CD signals were converted to mean residue ellipticity [Θ] = deg x cm^2 x $dmol^{-1}$ (Mol. Ellip.).

Fluorescent Intercalator Displacement (FID) assay

FID titrations were performed on a Perkin Elmer LS55 Luminescence equipped with thermostated cell holder. Spectra were acquired by using an excitation wavelength of 501 nm and recording the signal in the 520-680 nm emission range at 25 °C. A solution containing 0.62 μM of target DNA and 1.24 μM of thiazole orange (TO) was prepared in a 10 mm path-length cell and the corresponding fluorescence spectrum was acquired in the absence and presence of increasing concentrations of tested compounds in 10 mM Tris, 50 mM KCl, pH 7.5. The percentage of TO displacement was calculated as TO displacement = 100 - [(F/F_0) × 100], where F_0 is the fluorescence in the absence of ligand and F the fluorescence recorded at each point of titration. TO displacement was plotted as a function of compound concentration and the EC_{50} (half maximal effective concentration) was calculated. Each titration was repeated at least in triplicate.

Fluorescence melting studies

Fluorescence melting analyses were performed with Light Cycler 480 II Roche using an excitation source at 488 nm and recording the fluorescence emission at 520 nm. Samples (20 µl final volume) containing 0.25 µM DNA (strand concentration) were loaded on a 96-well plate in 10 mM LiOH; pH 7.5 with H_3PO_4, with 50 mM KCl and increasing concentrations of ligands. Samples were first heated and cooled in the 25-95 °C range at a rate of 0.1 °C s^{-1}. Then samples were maintained at 30 °C for 5 min before being slowly heated to 95 °C (1 °C/min) and annealed at a rate of 1 °C/min. For the analyses with double strands oligonucleotides, the two complementary strands were annealed before ligand addition. Melting temperatures were determined from the first derivatives of the melting profiles using the Roche LightCycler software. Each curve was repeated at least in triplicate and errors were ± 0.3 °C.

Crystallization

The DNA-drug complexes were crystallized at 296 K using the sitting drop vapor diffusion method from a solution containing 40% MPD, 50 mM Na Cacodylate pH=6.5, 150 mM sodium fluoride and 150 mM potassium fluoride, on the basis of a previously reported screening [33]. Drops were equilibrated against the same solution.

X-ray diffraction analyses

Coptisine was crystallized along with the human telomeric sequence Tel12 (5'-TAGGGTTAGGGT-3'). The crystal of the complex belonged to the space group $P4_32_12$ (tetragonal system) with cell dimensions a = b = 41.57 Å, c = 66.17 Å. The structure was refined to R_{factor} = 23.2% and $R_{free\ factor}$ = 25.9% to 1.55 Å resolution.

Data collection on crystals of the DNA-drug complexes were performed at 100 K, using as cryoprotectant the mother liquor solution, and the synchrotron radiation at the ID29 Beamline, ESRF Grenoble. Data were integrated and scaled using the program XDS [34]. The structure of the Coptisine complex was solved by the Molecular Replacement technique using the program Phaser [35] and the coordinates of the Tel12 G-quadruplex structure (PDB code 1K8P), [36] without all the heteroatoms, as a search model. The model was refined with the program Refmac5 [37] from the CCP4 program suite [38]. Manual rebuilding of the model was performed using the program Coot [39]. Data Collection and Refinement statistics are reported in ESI (Table S1). Final coordinates and structure factors have been deposited with the Protein Data Bank (PDB accession number 4P1D).

Molecular Modelling

The binding ability of Chelerythrine (iminium form) and Coptisine has been investigated toward Tel26 hybrid-1 (PDB code: 2HY9) [40], and wtTel26 hybrid-2 (PDB code: 2JPZ) [41] telomeric G-quadruplex structures. Both ligand molecules have been built by the Build module of Maestro [42]. The atomic electrostatic charges of the ligands were calculated at the B3LYP/6-311G**+ level of theory by fitting them to an electrostatic potential calculated using the Jaguar software [43]. Docking calculations were performed using Glide [44] with the DNA structures kept fixed in their original conformations throughout the docking procedures. Six different grids, two of them centered nearby the guanine platforms and the other ones nearby the lateral grooves, were prepared for each DNA folding. For each ligand DNA complex, poses obtained from all the grids were collected and submitted to a minimization procedure (MacroModel [45], OPLS2005 [46], maximum iteration 3000 cycles, 0.05 kJ/Å-mol convergence criterion) and then sorted as a function of their energy content. Only poses with energy no more than 5 kcal/mol above the minimum were selected. In the case of the results from grids centered nearby the guanine platforms, additional

molecular dynamics procedures were carried out (4.5 ns, T = 300 K, integration step 1.5 fs) by means of the Impact software [47].

Acknolwledgement

Ente Cassa di Risparmio di Firenze, Italy, is gratefully acknowledged for a grant to F.P (2014.0309). The PhD fellowships for R.R and S.D.R. were founded by Padova University.

References

1. (a) Rhodes, D., and Lipps, H. J. (2015) G-quadruplexes and their regulatory roles in biology, *Nucleic Acids Res. 43(18)*, 8627–8637; (b) Neidle, S. (2016) Quadruplex Nucleic Acids as Novel Therapeutic Targets, *J. Am. Chem. Soc. 59*, 5987–6011.

2. Sproviero, M., Fadock, K. L, Witham, A. A., and Manderville, R. A. (2015) Positional Impact of Fluorescently Modified G-Tetrads within Polymorphic Human Telomeric G-Quadruplex Structures, *ACS Chem. Biol. 10(5)*, 1311–1318.

3. (a) Düchler, M. (2012) G-quadruplexes: targets and tools in anticancer drug design, *J. Drug Targeting 20(5)*, 389–400; (b) Lu, Yu-Jing; Deng, Qiang; Hou, Jin-Qiang; Hu, Dong-Ping; Wang, Zheng-Ya; Zhang, Kun; Luyt, Leonard G.; Wong, Wing-Leung; Chow, Cheuk-Fai (2016) Molecular Engineering of Thiazole Orange Dye: Change of Fluorescent Signaling from Universal to Specific upon Binding with Nucleic Acids in Bioassay, *ACS Chem. Biol. 11(4)*, 1019–1029.

4. Ohnmacht, S. A., and Neidle, S. (2014) Small-molecule quadruplex-targeted drug discovery, *Bioorg. Med. Chem. Lett. 24*, 2602–2612.

5. (a) An, Na; Fleming, Aaron M.; Burrows, Cynthia J. (2016) Human Telomere G-Quadruplexes with Five Repeats Accommodate 8-Oxo-7,8-dihydroguanine by Looping out the DNA Damage, *ACS Chem. Biol. 11(2)*, 500–507. ; (b) Bidzinska, J., Cimino-Reale, G., Zaffaroni, N., and Folini, M. (2013) G-Quadruplex Structures in the Human Genome as Novel Therapeutic Targets, *Molecules 18(10)*, 12368–12395.

6. Maji, B., and Bhattacharya, S. (2014) Advances in the molecular design of potential anticancer agents via targeting of human telomeric DNA, *Chem. Commun. 50*, 6422–6438.

7. (a) Efferth, T., Li, P. C. H., Konkimalla, V. S. B., and Kaina, B. (2007) From traditional Chinese medicine to rational cancer therapy, *Trends Mol. Med. 13*, 353–361; (b) Harvey, A. L., Edrada-Ebel, R., and Quinn, R. J. (2015) The re-emergence of natural products for drug discovery in the genomics era, *Nat. Rev. Drug Discov. 14*, 111–129.

8. Khan, A. Y., and Kumar, G. S. (2015) Natural isoquinoline alkaloids: binding aspects to functional proteins, serum albumins, hemoglobin, and lysozyme, *Biophys. Rev. 7(4)*, 407–420.

9. (a) Raza, A., Aslam, B., Naseer, M. U., Ali, A., Majeed, W., and Shamshad-Ul-Hassan (2015) Antitumor activity of Berberine against breast cancer: A review, *Int. Res. J. Pharm. 6(2)*, 81–85; (b) Bashar, A. B. M. A., Hossan, M. S., Jahan, R., Nahain, A. A., Haque, A. K. M. M., and Rahmatullah, M. (2014) Berberine: A potential therapeutic candidate for breast cancer, *WJPPS 3(8)*, 1858–1869.

10. Kittakoop, P., Mahidol, C., and Ruchirawat, S. (2014) Alkaloids as important scaffolds in therapeutic drugs for the treatments of cancer, tuberculosis, and smoking cessation, *Curr. Top. Med. Chem. 14(2)*, 239–252.

11. Iranshahy, M., Quinn, R. J., and Iranshahi, M. (2014) Biologically active isoquinoline alkaloids with drug-like properties from the genus Corydalis, *RSC Adv. 4(31)*, 15900–15913.

12. Ni, W. J., Ding, H. H., and Tang, L. Q. (2015) Berberine as a promising anti-diabetic nephropathy drug: An analysis of its effects and mechanisms, *Eur. J. Pharmacol. 760*, 103–112.
13. (a) Tillhon, M., Guamàn Ortiz, L. M., Lombardi, P., and Scovassi, A. I. (2012) Berberine: new perspectives for old remedies, *Biochem. Pharmacol. 84*, 1260–1267; (b) El-Readi, M. Z., Eid, S. Y., Ashour, M. L., Tahrani, A., and Wink, M. (2013) Modulation of multidrug resistance in cancer cells by chelidonine and Chelidonium majus alkaloids, *Phytomedicine 20*, 282–294; (c) Kumar, A., Ekavali, Chopra, K., Mukherjee, M., Pottabathini, R., and Dhull, D. K. (2015) Current knowledge and pharmacological profile of berberine: An update, *Eur. J. Pharmacol. 761*, 288–297.
14. Chu, M., Xiao, R., Yin, Y., Wang, X., Chu, Z., Zhang, M., Ding, R., and Wang, Y. (2014) Berberine: A Medicinal Compound for the Treatment of Bacterial Infections, *Clin. Microbiol. 3(3)*, 1000150.
15. Lu, J. J., Bao, J. L., Chen, X. P., Huang, M., and Wang, Y. T. (2012) Alkaloids Isolated from Natural Herbs as the Anticancer Agents, *Evid. Based Complement Alternat. Med.*, 485042.
16. Sun, Y., Xun, K., Wang, Y., and Chen, X. (2009) A systematic review of the anticancer properties of berberine, a natural product from Chinese herbs, *Anticancer Drugs 20*, 757–769.
17. (a) Arora, A., Balasubramanian, C., Kumar, N., Agrawal, S., Ojha, R. P., and Maiti, S. (2008) Binding of berberine to human telomeric quadruplex - spectroscopic, calorimetric and molecular modeling studies, *FEBS J. 275(15)*, 3971–3983; (b) Bhadra, K., and Kumar, G. S. (2011) Interaction of berberine, palmatine, coralyne, and sanguinarine to quadruplex DNA: a comparative spectroscopic and calorimetric study, *Biochim. Biophys. Acta 1810*, 485–496.
18. (a) Bhowmik, D., Fiorillo, G., Lombardi, P., and Kumar, G. S. (2015) Recognition of human telomeric G-quadruplex DNA by berberine analogs: effect of substitution at the 9 and 13 positions of the isoquinoline moiety, *J. Mol. Recognit. 28(12)*, 722–730; (b) Ferraroni, M., Bazzicalupi, C., Papi, F., Fiorillo, G., Guamán-Ortiz, L. M., Nocentini, A., Scovassi, A. I., Lombardi, P., and Gratteri, P. (2016) Solution and Solid-State Analysis of Binding of 13-Substituted Berberine Analogues to Human Telomeric G-quadruplexes, *Chem. Asian J. 11*, 1107–1115; (c) Bhowmik, D., and Kumar, G. S. (2016) Recent Advances in Nucleic Acid Binding Aspects of Berberine Analogs and Implications for Drug Design, *Mini Rev. Med. Chem. 16(2)*, 104–119.
19. (a) Ghosh, S., Pradhan, S. K., Kar, A., Chowdhury, S., and Dasgupta, D. (2013) Molecular basis of recognition of quadruplexes human telomere and c-myc promoter by the putative anticancer agent sanguinarine, *Biochim. Biophys. Acta 1830(8)*, 4189–4201; (b) Pradhan, S. K., Dasgupta, D., and Basu, G. (2011) Human telomere d[$(TTAGGG)_4$] undergoes a conformational transition to the Na^+-form upon binding with sanguinarine in presence of K^+, *Biochem. Biophys. Res. Commun. 404*, 139–142.
20. Bessi, I., Bazzicalupi, C., Richter, C., Jonker, H. R. A., Saxena, K., Sissi, C., Chioccioli, M., Bianco, S., Bilia, A. R., Schwalbe, H., and Gratteri, P. (2012) Spectroscopic, molecular modeling, and NMR-spectroscopic investigation of the binding mode of the natural alkaloids berberine and sanguinarine to human telomeric G-quadruplex DNA, *ACS Chem. Biol. 7(6)*, 1109–1119.
21. (a) Wang, N., Feng, Y., Zhu, M., Tsang, C. M., Man, K., Tong, Y., and Tsao, S. W. (2010) Berberine induces autophagic cell death and mitochondrial apoptosis in liver cancer cells: The cellular mechanism, *J. Cell. Biochem. 111*, 1426–1436; (b) Mahata, S., Bharti, A. C., Shukla, S., Tyagi, A., Husain, S. A., and Das, B. C. (2011) Berberine modulates AP-1 activity to suppress HPV transcription and downstream signaling to induce growth arrest and apoptosis in cervical cancer cells, *Mol. Canc. 10*, 39; (c) Hou, Q., Tang, X., Liu, H., Tang, J., Yang, Y., Jing, X., Xiao, Q., Wang, W., Gou, X., and Wang, Z. (2011) Berberine induces cell death in human hepatoma cells in vitro by downregulating CD147, *Cancer Sci. 102(7)*, 1287–1292; (d) Hu, H. Y., Li, K. P., Wang, X. J., Liu, Y., Lu, Z. G., Dong, R. H., Guo, H. B., and Zhang, M. X. (2013) Set9, NF-κB, and microRNA-21 mediate berberine-induced apoptosis of human multiple myeloma cells, *Acta Pharmacol. Sin. 34*, 157–166; (e) Li, J., Gu, L., Zhang, H., Liu, T., Tian, D., Zhou, M., and Zhou, S. (2013) Berberine represses DAXX

gene transcription and induces cancer cell apoptosis, *Lab. Invest. 93*, 354–364; (f) Hamoud, R., Reichling, J., and Wink, M. (2014) Synergistic antibacterial activity of the combination of the alkaloid sanguinarine with EDTA and the antibiotic streptomycin against multidrug resistant bacteria, *J. Pharm. Pharmacol. 67(2)*, 264–273; (g) Gaziano, R., Moroni, G., Buè, C., Miele, M. T., Sinibaldi-Vallebona, P., and Pica, F. (2016) Antitumor effects of the benzophenanthridine alkaloid sanguinarine: Evidence and perspectives, *World J. Gastrointest. Oncol. 8(1)*, 30–39.

22. Yang, S., Xiang, J., Yang, Q., Li, Q., Zhou, Q., Zhang, X., Tang, Y., and Xu, G. (2010) Formation of Human Telomeric G-quadruplex Structures Induced by the Quaternary Benzophenanthridine Alkaloids: Sanguinarine, Nitidine, and Chelerythrine, *Chin. J. Chem. 28*, 771–780.

23. Ghosh, S., and Dasgupta, D. (2015) Quadruplex forming promoter region of c-myc oncogene as a potential target for a telomerase inhibitory plant alkaloid, chelerythrine, *Biochem. Biophys. Res. Commun. 459(1)*, 75–80.

24. Ghosh, S., Jana, J., Kar, R. K., Chatterjee, S., and Dasgupta, D. (2015) Plant Alkaloid Chelerythrine Induced Aggregation of Human Telomere Sequence—A Unique Mode of Association between a Small Molecule and a Quadruplex, *Biochemistry 54(4)*, 974–986.

25. Bai, L. P., Hagihara, M., Nakatani, K., and Jiang, Z. H. (2014) Recognition of Chelerythrine to Human Telomeric DNA and RNA G-quadruplexes, *Sci. Rep. 4*, 6767–6776.

26. (a) Yang, S., Xiang, J. F., Yang, Q. F., Zhou, Q. J., Zhang, X. F., Li, Q., Tang, Y. L., and Xu, G. Z. (2011) An important functional group, benzo[1,3]dioxole, of alkaloids induces the formation of the human telomeric DNA G-quadruplex, *Chin. Sci. Bull. 56(7)*, 613–617; (b) Ji, X., Sun, H., Zhou, H., Xiang, J., Tang, Y., and Zhao, C. (2012) The Interaction of Telomeric DNA and C-myc22 G-Quadruplex with 11 Natural Alkaloids, *Nucleic Acid Ther. 22(2)*, 127–136.

27. Lane, A.N., Chaires, J.B., Gray, R.D., and Trent, J.O. (2008) Stability and kinetics of G-quadruplex structures. *Nucleic Acids Res. 36.* 5482-5515

28. Dai, J., Carver, M., and Yang, D. (2008) Polymorphism of human telomeric quadruplex structures. *Biochimie 90*, 1172-1183.

29. Ferraroni, M., Bazzicalupi, C., Papi, F., and Gratteri, P. (2016) Double Helices Forming Unusual Binding Motifs: The Case of the Natural Alkaloids Coptisine and Chelerythrine. In *G-Quadruplex Structures, Formation and Role in Biology* (Santos, H., Ed.), 1st ed., pp 81–102, Nova Science Publishers, New York.

30. Collie, G. W., Campbell, N. H., and Neidle, S. (2015) Loop flexibility in human telomeric quadruplex small-molecule complexes, *Nucleic Acids Res. 43(10)*, 4785–4799.

31. Groom, C. R., Bruno, I. J., Lightfoot, M. P., and Ward, S. C. (2016) The Cambridge Structural Database, *Acta Cryst. B72*, 171–179.

32. Krauss, I. R., Ramaswamy, S., Neidle, S., Haider, S., and Parkinson, G. N. (2016) Structural Insights into the Quadruplex–Duplex 3’ Interface Formed from a Telomeric Repeat: A Potential Molecular Target, *J. Am. Chem. Soc. 138(4)*, 1226–1233.

33. Campbell, N. H., and Parkinson, G. N. (2007) Crystallographic studies of quadruplex nucleic acids, *Methods 43*, 252–263.

34. Kabsch, W. (2010) XDS, *Acta Cryst. D66*, 125–132.

35. McCoy, A. J., Grosse-Kunstleve, R. W., Adams, P. D., Winn, M. D., Storoni, L. C., and Read, R. J. (2007) Phaser crystallographic software, *J. Appl. Cryst. 40*, 658–674.

36. Parkinson, G. N., Lee, M. P., and Neidle, S. (2002) Crystal structure of parallel quadruplexes from human telomeric DNA, *Nature 417*, 876–880.

37. Murshudov, G. N., Skubák, P., Lebedev, A. A., Pannu, N. S., Steiner, R. A., Nicholls, R. A., Winn, M. D., Long, F., and Vagin, A. A. (2011) REFMAC5 for the refinement of macromolecular crystal structures, *Acta Cryst. D67*, 355–367.
38. Winn, M. D., Ballard, C. C., Cowtan, K. D., Dodson, E. J., Emsley, P., Evans, P. R., Keegan, R. M., Krissinel, E. B., Leslie, A. G. W., McCoy, A., McNicholas, S. J., Murshudov, G. N., Pannu, N. S., Potterton, E. A., Powell, H. R., Read, R. J., Vagin, A. A., and Wilson, K. S. (2011) Overview of the CCP4 suite and current developments, *Acta Cryst. D67*, 235–242.
39. Emsley, P., Lohkamp, B., Scott, W. G., and Cowtan, K. (2010) Features and development of Coot, *Acta Cryst. D66*, 486–501.
40. Dai, J., Punchihewa, C., Ambrus, A., Chen, D., Jones, R. A., and Yang, D. (2007) Structure of the intramolecular human telomeric G-quadruplex in potassium solution: a novel adenine triple formation, *Nucleic Acids Res. 35(7)*, 2440–2450.
41. Dai, J., Carver, M., Punchihewa, C., Jones, R. A., and Yang, D. (2007) Structure of the Hybrid-2 type intramolecular human telomeric G-quadruplex in K^+ solution: insights into structure polymorphism of the human telomeric sequence, *Nucleic Acids Res. 35(15)*, 4927–4940.
42. Maestro, version 9.2, Schrödinger, LLC, New York, NY, 2011.
43. Jaguar, version 7.8, Schrödinger, LLC, New York, NY, 2011.
44. Glide, version 5.7, Schrödinger, LLC, New York, NY, 2011.
45. MacroModel, version 9.9, Schrödinger, LLC, New York, NY, 2011.
46. Kaminski, G. A., Friesner, R. A., Tirado-Rives, J., and Jorgensen, W. L. (2001) Evaluation and Reparametrization of the OPLS-AA Force Field for Proteins via Comparison with Accurate Quantum Chemical Calculations on Peptides, *J. Phys. Chem. B 105(28)*, 6474-6487; Hornak, V., Abel, R., Okur, A., Strockbine, B., Roitberg, A., and Simmerling, C. (2006) Comparison of multiple Amber force fields and development of improved protein backbone parameters, *Proteins. 65(3)*, 712-725.
47. Impact version 7.1, Schrödinger, LLC, New York, NY, 2016.

Graphical Table of Contents